LETTER

https://doi.org/10.1038/s41586-018-0603-3

A slow-cycling LGR5 tumour population mediates basal cell carcinoma relapse after therapy

Adriana Sánchez-Danés[1], Jean-Christophe Larsimont[1], Mélanie Liagre[1], Eva Muñoz-Couselo[2,3], Gaëlle Lapouge[1], Audrey Brisebarre[1], Christine Dubois[1], Mariano Suppa[4], Vijayakumar Sukumaran[1], Véronique del Marmol[4], Josep Tabernero[2,3] & Cédric Blanpain[1,5]*

Basal cell carcinoma (BCC) is the most frequent cancer in humans and results from constitutive activation of the Hedgehog pathway[1]. Several Smoothened inhibitors are used to treat Hedgehog-mediated malignancies, including BCC and medulloblastoma[2]. Vismodegib, a Smoothened inhibitor, leads to BCC shrinkage in the majority of patients with BCC[3], but the mechanism by which it mediates BCC regression is unknown. Here we used two genetically engineered mouse models of BCC[4] to investigate the mechanisms by which inhibition of Smoothened mediates tumour regression. We found that vismodegib mediates BCC regression by inhibiting a hair follicle-like fate and promoting the differentiation of tumour cells. However, a small population of tumour cells persists and is responsible for tumour relapse following treatment discontinuation, mimicking the situation found in humans[5]. In both mouse and human BCC, this persisting, slow-cycling tumour population expresses LGR5 and is characterized by active Wnt signalling. Combining *Lgr5* lineage ablation or inhibition of Wnt signalling with vismodegib treatment leads to eradication of BCC. Our results show that vismodegib induces tumour regression by promoting tumour differentiation, and demonstrates that the synergy between Wnt and Smoothened inhibitors is a clinically relevant strategy for overcoming tumour relapse in BCC.

Vismodegib (GDC0449) is the first Smoothened inhibitor to be approved for the treatment of locally advanced and metastatic BCC. A small fraction of patients does not respond to vismodegib administration: their tumours continue to grow and do not show inhibition of the Hedgehog (Hh) signalling pathway during vismodegib treatment[3]. This type of vismodegib resistance is frequently associated with genetic mutations that render vismodegib unable to inhibit the Hh pathway[6,7]. Most patients treated with vismodegib experience clinical benefits[3]. However, many patients respond only partially: their tumours initially regress under therapy but relapse after vismodegib discontinuation[3,5]. The mechanisms by which vismodegib induces tumour regression and that underlie non-genetic resistance to vismodegib therapy are unknown.

To study the mechanisms by which vismodegib leads to BCC regression, we induced BCC in mice by deleting *Ptch1* or overexpressing the constitutive active form of *Smo* (*SmoM2*) in the epidermis using *Krt14-CreER*[8,9]. BCCs induced by conditional knockout of *Ptch1* (*Ptch1*^{cKO}) arise mainly from the upper hair follicle (infundibulum) whereas those induced by *SmoM2* originate from the interfollicular epidermis (IFE)[4,8]. Eight weeks after deletion of *Ptch1* by tamoxifen administration, mice showing fully formed BCCs were treated daily with vismodegib and analysed at different time points (Fig. 1a). A decrease in tumour burden was observed during the first 5 weeks of vismodegib treatment, followed by stabilization of tumour size from 5 to 12 weeks, together with the appearance of vismodegib-persistent lesions (Fig. 1b, c, Extended Data Fig. 1a–d). Vismodegib administration led to the conversion of the BCCs into pre-neoplastic lesions (hyperplasia and dysplasia), which persisted as drug-tolerant lesions (Fig. 1d, Extended Data Fig. 1e). These results show that vismodegib induces tumour shrinkage and the progressive appearance of drug-tolerant lesions.

Staining for active caspase-3 two weeks after vismodegib administration showed a similar number of apoptotic cells in treated and untreated mice (Fig. 1e, f, Extended Data Fig. 1f, g), indicating that apoptosis is not the main mechanism by which vismodegib induces BCC regression. As quiescence has been described as a mechanism of cancer resistance to therapy[10], we assessed the proportion of Ki67-positive tumour cells and observed a strong decrease in the proportion of proliferative cells in persistent lesions (Fig. 1g, h, Extended Data Fig. 1h, i), suggesting that quiescence contributes to the emergence of drug-tolerant cells.

Lgr5 is expressed by different epithelial stem cells, including hair follicle stem cells (HFSCs)[11], and is upregulated during BCC initiation[9] (Extended Data Fig. 2a). In situ hybridization (ISH) showed that *Lgr5* was highly expressed in untreated BCCs and its expression persisted, albeit at a lower level, in vismodegib-tolerant lesions (Fig. 2a, Extended Data Fig. 2b)

ISH for *Gli1*, a transcription factor that relays Hh signalling and a Hh target gene, demonstrated that *Gli1* was co-expressed with *Lgr5* before treatment and was strongly downregulated in all tumour cells upon vismodegib treatment (Fig. 2a–c, Extended Data Fig. 2b–d), consistent with the strong inhibition of Hh signalling by vismodegib. Drug-tolerant lesions did not present mutations in *Smo*, the most frequently mutated gene in vismodegib-resistant BCC[6,7] (Extended Data Fig. 2e), reinforcing the notion that the persistence of drug-tolerant lesions is not mediated by mutations that abrogate vismodegib sensitivity, as it occurs in vismodegib-resistant BCCs that continue to grow during treatment[6,7].

Relapse of BCC upon vismodegib discontinuation has been reported in human patients[5]. Discontinuation of vismodegib administration for 4 weeks in *Krt14*^{CreER};*Ptch1*^{cKO};*Lgr5*$^{DTR-GFP}$ mice[12] bearing drug-persistent lesions led to the re-growth of BCCs to their pre-treatment size. Moreover, re-administration of vismodegib to mice with relapsing BCCs led to tumour regression (Fig. 2d).

To determine whether the quiescent tumour cell population mediates tumour relapse, we performed BrdU pulse-chase label retention studies by administrating BrdU for 3 days in mice with BCC to label proliferative cells, and then monitored the labelling during 5 weeks of vismodegib treatment. We found BrdU label-retaining cells (LRCs) in LGR5$^+$ drug-tolerant lesions, suggesting that persisting tumour cells existed before vismodegib treatment and underwent a phenotype switch from a proliferative to a quiescent state (Fig. 2e, f). Upon discontinuation of vismodegib, relapsed tumours lost the LRCs (Fig. 2e, f), suggesting that quiescent LRCs actively proliferated, diluting the BrdU. To test this possibility directly, we performed BrdU–EdU double-labelling studies. Administration of EdU during vismodegib discontinuation led to EdU incorporation in the majority of the LGR5$^+$BrdU$^+$ LRCs (Fig. 2g,

[1]Laboratory of Stem Cells and Cancer, Université Libre de Bruxelles, Brussels, Belgium. [2]Vall d'Hebron University Hospital, Universitat Autònoma de Barcelona, Barcelona, Spain. [3]Vall d'Hebron Institute of Oncology (VHIO), Universitat Autònoma de Barcelona, Barcelona, Spain. [4]Department of Dermatology, Erasme Hospital, Université Libre de Bruxelles, Brussels, Belgium. [5]WELBIO, Université Libre de Bruxelles, Brussels, Belgium. *e-mail: cedric.blanpain@ulb.ac.be

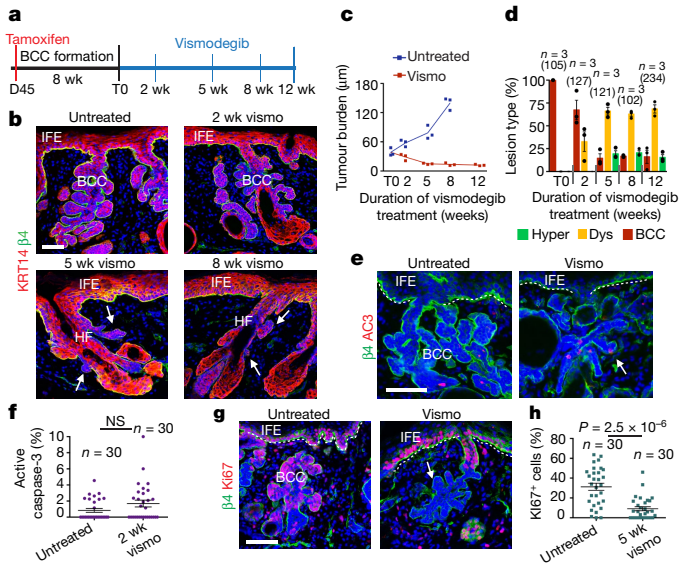

Fig. 1 | Slow-cycling tumour cells persist following vismodegib treatment in mouse *Ptch1*^{cKO}-derived BCCs. a, Protocol for tumour induction and vismodegib (vismo) administration. **b**, Immunostaining for KRT14 and β4-integrin (β4) in ventral skin from *Ptch1*^{cKO} mice. HF, hair follicle. **c**, Tumour burden (total area occupied by tumours divided by the length of the analysed epidermis) in untreated and vismodegib-treated mice ($n = 3$ mice analysed per time point and condition). Squares show data for individual mice, lines show mean. See Source Data. **d**, Quantification of lesion type (mean ± s.e.m.) upon vismodegib treatment ($n = 3$ mice, total number of lesions analysed per time point indicated in parentheses). Hyper, hyperplasia; dys, dysplasia. **e**, Immunostaining for active caspase-3 (AC3) and β4-integrin. **f**, Percentage of AC3$^+$ tumour cells (mean ± s.e.m.) in untreated and vismodegib-treated mice ($n = 30$ lesions analysed from 3 mice). Two-sided *t*-test. **g**, Immunostaining for Ki67 and β4-integrin. **h**, Percentage of Ki67$^+$ tumour cells (mean ± s.e.m.) in untreated and vismodegib-treated mice ($n = 30$ lesions analysed from 3 mice). Two-sided *t*-test. Hoechst nuclear staining in blue; scale bars, 50 μm. Dashed line in **e**, **g** delineates basal lamina. Arrows in **b**, **e**, **g** indicate vismodegib-persistent lesions.

Extended Data Fig. 2f, g), further demonstrating that the quiescent LRCs re-enter cell cycle and proliferate to contribute to tumour relapse.

To determine whether quiescence promotes the persistence of the vismodegib-tolerant lesions, we assessed whether increased epidermal proliferation decreased the number of drug-tolerant lesions. Mice bearing LGR5$^+$ persistent lesions were treated for 2 weeks with vismodegib in combination with 12-*O*-tetradecanoylphorbol-13-acetate (TPA) or retinoic acid, two drugs that promote epidermal proliferation. Combined administration of vismodegib and TPA or retinoic acid promoted proliferation, which led to the elimination of LGR5$^+$ persistent lesions (Extended Data Fig. 2h–j), demonstrating that when persistent slow-cycling cells are forced to proliferate they become sensitive to vismodegib and are eliminated.

We isolated the persistent tumour cells using fluorescence-activated cell sorting (FACS), by combining LGR5–GFP with LRIG1, which does not co-localize with LGR5 in resting hair follicles[13] (Extended Data Fig. 2k–m). Upon vismodegib administration, the proportion of LGR5$^+$LRIG1$^+$ cells decreased and there was an increase in the LRG5$^-$LRIG1$^+$ population (Extended Data Fig. 2m, n).

We then characterized the gene signature of FACS-isolated LGR5$^+$LRIG1$^+$ and LRG5$^-$LRIG1$^+$ tumour cell populations from untreated BCCs using microarray analysis. It has been shown that, during BCC initiation, IFE and infundibulum cells targeted by *Ptch1*^{cKO} or *SmoM2* are reprogrammed into fates resembling those of embryonic hair follicle progenitor (EHFP) cells and adult hair follicles in a Wnt-dependent manner[9,14]. Genes that were upregulated in LGR5$^+$LRIG1$^+$ tumour cells compared to LRG5$^-$LRIG1$^+$ tumour cells (LGR5$^+$ BCC signature) overlapped significantly with the EHFP signature[15] (23.3%), resting HFSC signature[16] (16.4%) and LGR5$^+$ hair follicle signature[17] (44.2%) (Fig. 3a, Extended Data Fig. 3a). The LGR5$^+$ BCC signature included genes downstream of the Hh signalling pathway, such as *Ptch1*, *Ptch2* and *Hhip*, genes involved in the Wnt signalling pathway, such as *Lgr5*, *Fzd2* and *Lef1*, transcription factors expressed by EHFPs, such as *Runx1* and *Lhx2*, and genes expressed by HFSCs, such as *Tbx1* and *Foxc1* (Extended Data Fig. 2b). Immunostaining for LEF1, LHX2, CUX1, TBX1, and ALCAM in *Ptch1*^{cKO}-induced BCCs confirmed the increased expression of these Wnt signalling, EHFP and HFSC markers in LGR5$^+$ tumour cells (Extended Data Fig. 3c).

To assess whether the LRG5$^-$LRIG1$^+$ population represents a differentiated part of the BCC, we defined genes that were upregulated in LRG5$^-$LRIG1$^+$ tumour cells compared to LGR5$^+$LRIG1$^+$ tumour cells (LGR5$^-$ signature). Notably, the LGR5$^-$ signature overlapped significantly with previously reported LRIG1[13] and IFE[16] signatures, including markers of IFE or infundibulum differentiation such as *Ovol1*, *Notch3*, *Defb6*, *Krt1* and *Krt10* (Extended Data Fig. 3d, e). PCR analysis performed on FACS-isolated LGR5$^+$LRIG1$^+$ and LGR5$^-$LRIG1$^+$ tumour cells confirmed that both populations had *Ptch1* deletion, and staining for the proliferation marker Ki67 showed that the LRG5$^+$LRIG1$^+$ population was more proliferative than the LGR5$^-$LRIG1$^+$ population (Extended Data Fig. 3f, g).

To directly assess whether LGR5$^-$LRIG1$^+$ cells were more differentiated than LGR5$^+$LRIG1$^+$ cells, we performed transplantation assays of FACS-isolated tumour cell populations from *Krt14*^{CreER};*Ptch1*^{cKO};*Lgr5*$^{DTR-GFP}$ and *Krt14*^{CreER};*Ptch1*^{cKO};*Trp53*^{cKO};*Lgr5*$^{DTR-GFP}$ mice, which grow faster and form bigger tumours[18]. Groups of cells resembling early BCC and expressing KRT14, LGR5 and LRIG1 were observed only upon transplantation of LGR5$^+$LRIG1$^+$ cells from *Trp53*^{cKO} mice (in three out of seven mice). By contrast, no tumour cells were observed following the transplantation of LGR5$^-$LRIG1$^+$ cells from *Trp53*^{cKO} BCCs or in the absence of *Trp53* deletion (Extended Data Fig. 4a, b). Tumours found after transplantation of LGR5$^+$LRIG1$^+$ cells mimicked the different cell types present in BCCs: LGR5$^+$LRIG1$^+$, LGR5$^-$LRIG1$^+$ and cells with a flat differentiated morphology expressing keratin-10 (KRT10) (Extended Data Fig. 4b, c). Together, these results show that BCCs contain a more stem-like or progenitor-like tumour cell population (LGR5$^+$LRIG1$^+$) and a more differentiated population (LGR5$^-$LRIG1$^+$) of tumour cells. Immunostaining for the primary cilia marker ARL13B and the coactivator MKL1 showed that neither loss of primary cilia[19] nor serum response factor (SRF)–MKL1 activation[20] is involved in the drug-tolerant phenotype described here (Extended Data Fig. 5a–d).

To define the molecular mechanisms by which vismodegib promotes tumour shrinkage and appearance of drug-tolerant lesions, we compared the transcriptional profiles of FACS-isolated LGR5$^+$LRIG1$^+$ and LGR5$^+$LRIG1$^-$ tumour cells from untreated BCCs and mice that received vismodegib for 8 weeks. We found that the overlap between the LGR5$^+$LRIG1$^+$ signature and the EHFP[15], LGR5$^+$ hair follicle[17] and resting HFSC[16] signatures was considerably lower in vismodegib-treated cells than in untreated cells (Fig. 3a, b). Vismodegib treatment induced a strong decrease in the expression of Hh target genes such as *Gli1*, *Gli2*, *Ptch1*, *Ptch2* and *Hhip* (Fig. 3c). Only a small part of the reduction in overlap between the vismodegib-treated and EHFP signatures was driven by Hh target genes such as *Hhip1*, *Ptch2* and *Gli1*, and the reduction in overlap between the HFSC and vismodegib-treated signatures was not mediated by Hh target genes as the HFSC signature was obtained in the resting state, when Hh signalling is not active[16]. Genes found in the EHFP and HFSC signatures, such as *Runx1*, *Lhx2*, *Lgr5*, *Alcam* and *Tbx1* were also downregulated following vismodegib administration at the mRNA and protein levels (Fig. 3c and Extended Data Fig. 6a).

The overlap between the LGR5$^+$LRIG1$^+$ signature and the infundibulum[13] and IFE[16] signatures increased considerably upon vismodegib treatment, with genes such as *Ovol1*, *Notch3*, *Plet1*, *Defb1*, *Defb6*, *Krt1* and *Krt10* being strongly upregulated after vismodegib treatment (Fig. 3d–f, Extended Data Fig. 6b), indicating that vismodegib

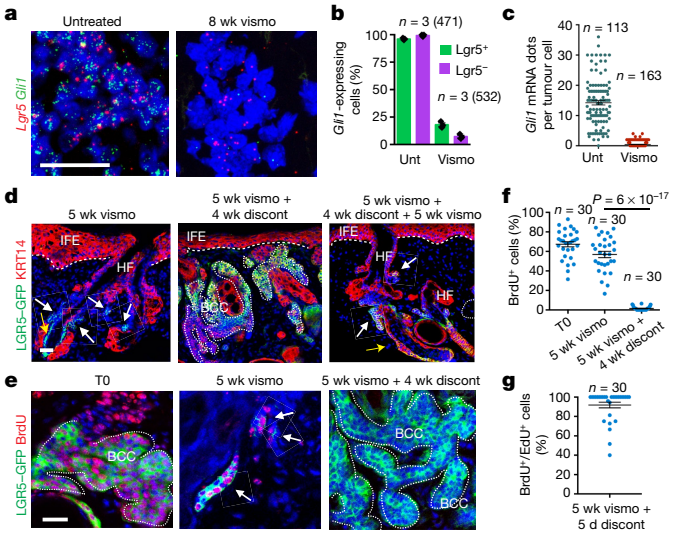

Fig. 2 | Slow-cycling LGR5$^+$ LRCs mediate tumour relapse following discontinuation of vismodegib. a, ISH for *Lgr5* (red) and *Gli1* (green) in untreated and treated tumour cells from *Krt14*^{CreER};*Ptch1*^{cKO} mice. **b**, Percentage of tumour cells (LGR5$^+$ and LGR5$^-$) that express *Gli1* (mean ± s.e.m.; $n = 3$ *Krt14*^{CreER};*Ptch1*^{cKO};*Lgr5*$^{DTR\text{-}GFP}$ mice, total number of cells analysed indicated in parentheses). **c**, Distribution of the number of *Gli1* mRNA dots per tumour cell with and without treatment (unt) (mean ± s.e.m.; $n = 113$ and 163 total tumour cells from 3 *Krt14*^{CreER};*Ptch1*^{cKO};*Lgr5*$^{DTR\text{-}GFP}$ mice per condition and time point). **d**, Immunostaining for LGR5–GFP and KRT14 in *Ptch1*^{cKO} ventral skin following vismodegib treatment, discontinuation and vismodegib re-administration. Three independent experiments per condition were analysed and showed similar results. **e**, Immunostaining for LGR5–GFP and BrdU following BrdU administration and after 5 and 9 weeks of chase in *Ptch1*^{cKO}-induced BCCs. **f**, **g**, Proportions of LGR5$^+$ tumour cells presenting BrdU labelling at T0, after vismodegib treatment and discontinuation (**f**) and BrdU$^+$EdU$^+$ double-positive tumour cells 5 days after vismodegib discontinuation (**g**) in *Ptch1*^{cKO}-induced BCCs (mean ± s.e.m.; $n = 30$ lesions analysed from 3 mice per condition). Two-sided *t*-test (**f**, **g**). Hoechst nuclear staining in blue; scale bars, 25 μm. Dashed lines delineate basal lamina; white arrows indicate vismodegib-persistent lesions; yellow arrows indicate hair follicle LGR5$^+$ cells. RA, retinoic acid.

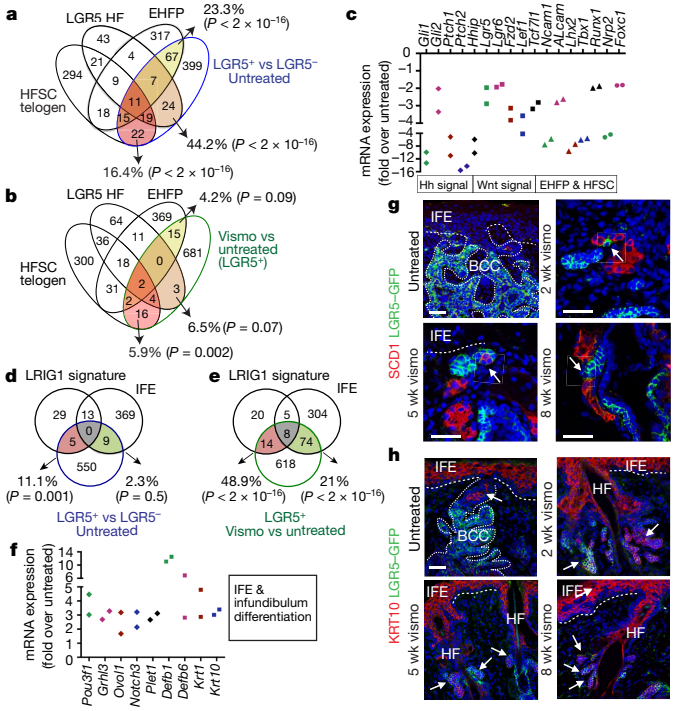

Fig. 3 | Vismodegib promotes BCC differentiation. a, **b**, Venn diagrams showing the similarities and the differences from two independent microarray experiments between genes upregulated more than twofold in LGR5$^+$LRIG1$^+$ versus LGR5$^-$LRIG1$^+$ cells (**a**) or in LGR5$^+$LRIG1$^+$ cells treated with vismodegib versus untreated (**b**) with the telogen HFSC signature[16], hair follicle LGR5-expressing cell signature[17] and EHFP signature[15]. **c**, mRNA expression of hair follicle genes downregulated in LGR5$^+$LRIG1$^+$ cells after 8 weeks of vismodegib administration ($n = 2$ independent microarray experiments). **d**, **e**, Venn diagrams showing the similarities and differences between genes that were differentially upregulated more than twofold from two independent microarray experiments in untreated LGR5$^+$LRIG1$^+$ versus LGR5$^-$LRIG1$^+$ cells (**d**) or in untreated versus vimodegib-treated LGR5$^+$LRIG1$^+$ tumour cells (**e**) compared to IFE[16] and LRIG1[13] signatures. **f**, mRNA expression of IFE and infundibulum genes that were upregulated in LGR5$^+$LRIG1$^+$ cells after 8 weeks of vismodegib administration ($n = 2$ independent microarray experiments). **g**, Immunostaining for LGR5–GFP and SCD1 in untreated and vismodegib-treated *Ptch1*^{cKO}-induced BCCs. Arrow indicates areas of sebaceous gland differentiation. **h**, Immunostaining for LGR5–GFP and KRT10 in untreated and vismodegib-treated *Ptch1*^{cKO} mice. Arrow indicates differentiation of LGR5$^+$ tumour cells into KRT10-expressing cells. Three independent experiments per condition were analysed with similar results (**g**, **h**). Hoechst nuclear staining in blue; scale bars, 50 μm. Dashed line delineates basal lamina. *P* values calculated using hypergeometric test for each intersection of two subsets of genes with phyper function in R software (**a**, **b**, **d**, **e**).

promotes the differentiation of BCC into IFE- and infundibulum-like cells, possibly through a Notch-dependent mechanism[21].

LRIG1$^+$ stem cells give rise to infundibulum and sebaceous gland under homeostatic conditions[13]. We performed staining for sebaceous gland markers (SCD1 and adipophilin) and lipids (Oil Red O). Whereas sebaceous cysts were visible in the dermis under untreated conditions, cells expressing sebaceous gland markers were localized within the tumour mass after two weeks of vismodegib treatment and adjacent to the neoplastic lesions after five or eight weeks of treatment (Fig. 3g, Extended Data Fig. 6c, d). We studied the expression of KRT10 and *Defensin-β6* (*Defb6*), which are normally expressed in infundibulum and IFE cells. Upon vismodegib administration, KRT10 and *Defb6* were strongly upregulated in tumour cells (Fig. 3h, Extended Data Fig. 6e), consistent with vismodegib inducing tumour differentiation towards a sebaceous gland/infundibulum/IFE-like fate in *Ptch1*^{cKO}-derived BCCs.

We then assessed whether vismodegib also promotes differentiation of BCC into IFE in *SmoM2*-induced BCC. Upon vismodegib administration, *SmoM2*-expressing cells connected to normal differentiating IFE cells expressed high levels of the IFE differentiation marker keratin-1 (KRT1) (Extended Data Fig. 6f). We studied the effect of vismodegib administration on the survival and morphology of the *SmoM2* clones during BCC initiation. Two weeks after *SmoM2* expression, mice were treated daily with vismodegib for six weeks (Extended Data Fig. 7a). Vismodegib administration led to a progressive loss of *SmoM2*-expressing clones in comparison to untreated conditions and to the emergence of clones with normal differentiation, with only a small proportion of the clones progressing into hyperplasia and dysplasia (Extended Data Fig. 7b–d). The normally differentiated clones observed during vismodegib treatment were positive for the differentiation marker KRT10 but did not express LHX2, an HFSC marker that is found in hyperplasias and dysplasias (Extended Data Fig. 7e, f), indicating that vismodegib administration inhibits oncogene-induced hair follicle reprograming, promotes differentiation of *SmoM2*-expressing cells into an IFE-like fate and prevents BCC initiation.

To assess whether LGR5$^+$ tumour cells consist of heterogeneous populations in terms of proliferation and differentiation, we isolated LGR5$^+$LRIG1$^+$ tumour cells on the basis of expression of the proliferation marker CD71[10] two weeks after vismodegib administration, when both persistent cells and cells that are responsive to vismodegib co-exist. The CD71$^+$ population expressed higher levels of proliferation (*Ki67* and *Aurka*) and differentiation markers (*Krt1*, *Krt10* and

Scd1) (Extended Data Fig. 7g), indicating that the more proliferative tumour cells are more prone to vismodegib-induced differentiation. Immunostaining for the differentiation marker KRT10 in LGR5$^+$ tumour cells after BrdU label-retention followed by two weeks of vismodegib administration showed that the majority of BrdU-labelled cells were negative for KRT10, whereas KRT10 was observed in non-LRCs or in LRCs in which the BrdU signal was lower owing to its dilution following cell division (Extended Data Fig. 7h). These results support the notion that vismodegib induces a higher rate of differentiation in the drug-responsive tumour population that actively cycles.

To determine the relevance of our findings to human patients, we analysed biopsies from four patients with locally advanced BCCs before, during or immediately after discontinuation of vismodegib treatment. Vismodegib did not eradicate all tumour cells in these patients, and small tumorigenic lesions expressing *LGR5* persisted despite the administration of vismodegib for months (Extended Data Fig. 8a–c). ISH for *GLI1* and quantification of *GLI1* mRNA dots per tumour cell before, after or during vismodegib treatment showed that there was almost no *GLI1* expression in samples from patients during vismodegib treatment but few more *GLI1*-expressing cells were found shortly after discontinuation of vismodegib treatment (Extended Data Fig. 8c, d), indicating that vismodegib administration efficiently inhibits Hh signalling in these drug-persistent lesions. Ki67 immunohistochemistry showed that vismodegib-persistent lesions were more quiescent than untreated BCC cells, and vismodegib induced the expression of the differentiation marker KRT10 in human tumour cells (Extended Data Fig. 8e, f). Notably, patients 1 and 2 relapsed 6 and 9 months after treatment discontinuation, respectively, and patient 4 had previously relapsed after vismodegib discontinuation, showing that vismodegib-mediated tumour cell persistence is fully reversible upon drug withdrawal and re-inducible upon a new cycle of vismodegib treatment (Extended Data Fig. 8a). Together, these results show that drug-tolerant lesions exist in human BCC, characterized by the expression of LGR5 and relative quiescence.

To assess whether LGR5$^+$ cells mediate tumour growth, we lineage-ablated LGR5$^+$ tumour cells by administrating diphtheria toxin for 10 days to *Krt14*^{CreER};*Ptch1*^{cKO};*Lgr5*$^{DTR\text{-}GFP}$ mice and for 15 days to *Krt14*^{CreER};*Rosa*^{SmoM2};*Lgr5*$^{DTR\text{-}GFP}$ mice (Extended Data Fig. 9a). Diptheria toxin treatment could not be extended because LGR5 deletion is toxic to normal liver cells[12]. Diptheria toxin administration led to a substantial elimination of the tumour mass in both BCC models (80% of the initial tumour mass) and to almost total elimination of LGR5-expressing cells in *Ptch1*^{cKO}-induced BCC (Extended Data Fig. 9b–g), further demonstrating the importance of LGR5$^+$ tumour cells to sustain BCC growth and maintenance.

To determine whether vismodegib administration together with *Lgr5* lineage ablation can eliminate the LGR5-expressing drug-tolerant lesions that are responsible for tumour relapse, we administrated diphtheria toxin for five consecutive days in combination with vismodegib to *Krt14*^{CreER};*Ptch1*^{cKO};*Lgr5*$^{DTR\text{-}GFP}$ mice bearing persistent lesions (Extended Data Fig. 9h). *Lgr5* ablation combined with vismodegib administration led to almost total (99.5%) elimination of the persistent LGR5-expressing tumour cells (Extended Data Fig. 9i–k). We did not observe reappearance of LGR5$^+$ cells from the vast majority (94%) of the initial LGR5$^+$ persistent tumorigenic lesions 15 days after discontinuation of treatment with diphtheria toxin and vismodegib (Extended Data Fig. 9i, k, l), whereas HFSCs were replenished by LGR5-expressing cells as previously reported[22], indicating that there is little plasticity within the LGR5$^-$LRIG1$^+$ BCC cells to revert to LGR5$^+$ tumour cells after treatment with diphtheria toxin and vismodegib. The therapeutic benefit of *Lgr5* ablation in BCC is reminiscent of the effect of *Lgr5* ablation in a mouse model of colorectal cancer, in which *Lgr5* ablation prevents metastasis, and in human colorectal cancer organoids, in which *Lgr5* ablation promotes tumour regression and synergises with chemotherapy[23,24].

Lgr5 has been identified as a Wnt target gene, and acts as a co-receptor for R-spondin, positively regulating the Wnt signalling pathway[11].

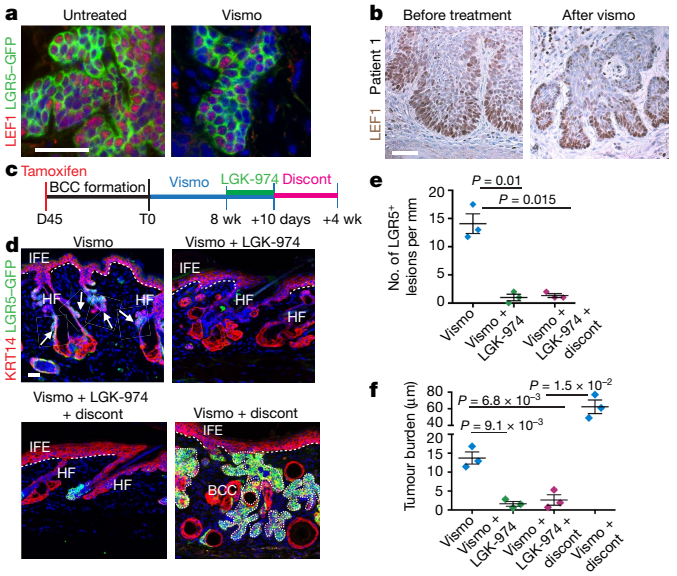

Fig. 4 | Dual Hh and Wnt inhibition eliminates vismodegib-persistent LGR5$^+$ tumour cells. a, Immunostaining for LGR5–GFP and LEF1 in untreated and vismodegib-treated *Ptch1*^{cKO} mice. **b**, Immunohistochemistry for LEF1 in biopsies from a patient before and after vismodegib treatment. **c**, Protocol for dual Hh and Wnt inhibition followed by treatment discontinuation. **d**, Immunostaining for LGR5–GFP and KRT14 upon vismodegib administration, dual inhibition of Wnt and Hh pathways and following discontinuation in *Ptch1*^{cKO}-derived BCCs. **e**, Number of LGR5$^+$ tumorigenic lesions per length of epidermis upon treatment and treatment discontinuation in *Ptch1*^{cKO}-induced BCCs (mean ± s.e.m.; $n = 3$ mice, 3 mm of skin analysed per mouse). Two-sided *t*-test. **f**, Quantification of the tumour burden upon treatment and treatment discontinuation in mice with *Ptch1*^{cKO}-induced BCCs (mean ± s.e.m.; $n = 3$ mice). See Source Data. Two-sided *t*-test. Three independent experiments per condition were analysed showing similar results (**a**) and two technical replicates were performed for each sample showing similar results (**b**). Hoechst nuclear staining in blue; scale bars, 50 µm. Dashed line delineates basal lamina; arrows indicate vismodegib-persistent lesions.

Administration of vismodegib decreased but did not abolish the expression of different members of the Wnt signalling pathway (Fig. 3c). Immunostaining for LEF1, a transcription factor that relays Wnt signalling and is a Wnt target gene in BCCs[9], and ISH for *Axin2*, another Wnt target gene, showed that both LEF1 and *Axin2* were expressed in LGR5$^+$ persistent lesions from mice and humans (Fig. 4a, b, Extended Data Fig. 10a, b), indicating that LGR5$^+$ persistent tumour cells are characterized by active Wnt signalling.

To assess whether dual Wnt and Hh inhibition can promote the elimination of LGR5$^+$ persistent tumour cells, we administered LGK-974, a porcupine Wnt inhibitor[25], and vismodegib for 10 consecutive days to *Ptch1*^{cKO} mice bearing LGR5$^+$ persistent lesions (Fig. 4c). Combined Wnt and Hh inhibition resulted in the disappearance of LEF1 expression consistent with efficient Wnt inhibition, the elimination of the vast majority (93%) of initial LGR5$^+$ drug-tolerant lesions and a substantial (87%) decrease in the tumour burden compared to vismodegib treatment alone (Fig. 4d–f, Extended Data Fig. 10c). We found no significant reduction in tumour burden after administration of the Wnt inhibitor alone, showing that although Wnt inhibition can block BCC initiation[9,14] it is not efficient as a monotherapy to induce clinically relevant BCC regression (Extended Data Fig. 10d–f), We then investigated whether rare residual tumour cells could lead to tumour relapse upon discontinuation of dual Wnt and Hh inhibition. Four weeks after discontinuation, which corresponds to the time that it takes for drug-tolerant lesions to regrow to their initial size upon vismodegib discontinuation, no tumour relapse was observed, as shown by the stable number of LGR5$^+$ tumour lesions and tumour burden (Fig. 4d–f).

Together, these results show that the synergy between Hh and Wnt inhibition in BCC leads to the elimination of the vast majority of LGR5$^+$ persistent tumour cells and thereby prevents tumour relapse.

In summary, we have shown that vismodegib induces BCC regression by promoting tumour differentiation and have identified a quiescent tumour cell population expressing LGR5 that persists after vismodegib treatment in different mouse models and human patients, promoting BCC relapse upon treatment discontinuation (Extended Data Fig. 11). The non-genetic mechanism of drug resistance described here differs from the previously described mutations in *Smo* or other genes that render cells insensitive to vismodegib treatment[6,7,19,20]. Administration of vismodegib promotes a switch from a proliferative state that fosters tumour growth to a tumour state characterized by Hh inhibition and slow-cycling properties that is fully reversible upon drug withdrawal and re-inducible upon a new cycle of vismodegib treatment. These persistent LGR5$^+$ tumour cells present residual Wnt signalling activity in both mouse and human BCCs and could be eliminated by dual Wnt and Hh inhibition, leading to tumour eradication in the majority of BCCs (Extended Data Fig. 11). Dual Wnt and Hh inhibition constitutes a clinically relevant strategy to avoid BCC relapse that might also be effective against other cancers, such as medulloblastoma, that are characterized by activation of Hh and Wnt signalling[26].

Online content

Any methods, additional references, Nature Research reporting summaries, source data, statements of data availability and associated accession codes are available at https://doi.org/10.1038/s41586-018-0603-3.

Received: 3 July 2017; Accepted: 16 August 2018;
Published online 8 October 2018.

1. Epstein, E. H. Basal cell carcinomas: attack of the hedgehog. *Nat. Rev. Cancer* **8**, 743–754 (2008).
2. Basset-Seguin, N., Sharpe, H. J. & de Sauvage, F. J. Efficacy of Hedgehog pathway inhibitors in basal cell carcinoma. *Mol. Cancer Ther.* **14**, 633–641 (2015).
3. Sekulic, A. et al. Efficacy and safety of vismodegib in advanced basal-cell carcinoma. *N. Engl. J. Med.* **366**, 2171–2179 (2012).
4. Kasper, M., Jaks, V., Hohl, D. & Toftgård, R. Basal cell carcinoma - molecular biology and potential new therapies. *J. Clin. Invest.* **122**, 455–463 (2012).
5. Tang, J. Y. et al. Inhibition of the hedgehog pathway in patients with basal-cell nevus syndrome: final results from the multicentre, randomised, double-blind, placebo-controlled, phase 2 trial. *Lancet Oncol.* **17**, 1720–1731 (2016).
6. Atwood, S. X. et al. Smoothened variants explain the majority of drug resistance in basal cell carcinoma. *Cancer Cell* **27**, 342–353 (2015).
7. Sharpe, H. J. et al. Genomic analysis of smoothened inhibitor resistance in basal cell carcinoma. *Cancer Cell* **27**, 327–341 (2015).
8. Youssef, K. K. et al. Identification of the cell lineage at the origin of basal cell carcinoma. *Nat. Cell Biol.* **12**, 299–305 (2010).
9. Youssef, K. K. et al. Adult interfollicular tumour-initiating cells are reprogrammed into an embryonic hair follicle progenitor-like fate during basal cell carcinoma initiation. *Nat. Cell Biol.* **14**, 1282–1294 (2012).
10. Brown, J. A. et al. TGF-β-induced quiescence mediates chemoresistance of tumor-propagating cells in squamous cell carcinoma. *Cell Stem Cell* **21**, 650–664.e8 (2017).
11. Barker, N., Tan, S. & Clevers, H. Lgr proteins in epithelial stem cell biology. *Development* **140**, 2484–2494 (2013).
12. Tian, H. et al. A reserve stem cell population in small intestine renders Lgr5-positive cells dispensable. *Nature* **478**, 255–259 (2011).
13. Page, M. E., Lombard, P., Ng, F., Göttgens, B. & Jensen, K. B. The epidermis comprises autonomous compartments maintained by distinct stem cell populations. *Cell Stem Cell* **13**, 471–482 (2013).
14. Yang, S. H. et al. Pathological responses to oncogenic Hedgehog signaling in skin are dependent on canonical Wnt/β3-catenin signaling. *Nat. Genet.* **40**, 1130–1135 (2008).
15. Rhee, H., Polak, L. & Fuchs, E. Lhx2 maintains stem cell character in hair follicles. *Science* **312**, 1946–1949 (2006).
16. Blanpain, C., Lowry, W. E., Geoghegan, A., Polak, L. & Fuchs, E. Self-renewal, multipotency, and the existence of two cell populations within an epithelial stem cell niche. *Cell* **118**, 635–648 (2004).
17. Latil, M. et al. Cell-type-specific chromatin states differentially prime squamous cell carcinoma tumor-initiating cells for epithelial to mesenchymal transition. *Cell Stem Cell* **20**, 191–204.e5 (2017).
18. Sánchez-Danés, A. et al. Defining the clonal dynamics leading to mouse skin tumour initiation. *Nature* **536**, 298–303 (2016).
19. Zhao, X. et al. A transposon screen identifies loss of primary cilia as a mechanism of resistance to SMO inhibitors. *Cancer Discov.* **7**, 1436–1449 (2017).
20. Whitson, R. J. et al. Noncanonical hedgehog pathway activation through SRF-MKL1 promotes drug resistance in basal cell carcinomas. *Nat. Med.* **24**, 271–281 (2018).
21. Eberl, M. et al. Tumor architecture and notch signaling modulate drug response in basal cell carcinoma. *Cancer Cell* **33**, 229–243.e4 (2018).
22. Hoeck, J. D. et al. Stem cell plasticity enables hair regeneration following Lgr5$^+$ cell loss. *Nat. Cell Biol.* **19**, 666–676 (2017).
23. de Sousa e Melo, F. et al. A distinct role for Lgr5$^+$ stem cells in primary and metastatic colon cancer. *Nature* **543**, 676–680 (2017).
24. Shimokawa, M. et al. Visualization and targeting of LGR5$^+$ human colon cancer stem cells. *Nature* **545**, 187–192 (2017).
25. Liu, J. et al. Targeting Wnt-driven cancer through the inhibition of Porcupine by LGK974. *Proc. Natl Acad. Sci. USA* **110**, 20224–20229 (2013).
26. Northcott, P. A. et al. Medulloblastomics: the end of the beginning. *Nat. Rev. Cancer* **12**, 818–834 (2012).

Acknowledgements We thank J.-M. Vanderwinden and M. Martens for help with confocal microscopy. C.B. is an investigator of WELBIO. A.S.-D. and J.-C.L. are supported by fellowships from the FNRS and FRIA, respectively. This work was supported by the FNRS, the Marian Family, the ULB fondation, the foundation Baillet Latour, and a consolidator grant from the European Research Council.

Author contributions A.S.-D. and C.B. designed the experiments, performed data analysis and wrote the manuscript; A.S.-D. performed most of the biological experiments; J.-C.L, G.L. and V.S. helped with *Lgr5* ablation experiments; M.L. performed immunostaining; C.D. performed FACS; E.M.-C., M.S., V.d.M. and J.T. provided patient samples; and A.B. performed GSEA.

Competing interests C.B. is a consultant at Genentech (San Francisco, USA).

Additional information
Extended data is available for this paper at https://doi.org/10.1038/s41586-018-0603-3.
Supplementary information is available for this paper at https://doi.org/10.1038/s41586-018-0603-3.
Reprints and permissions information is available at http://www.nature.com/reprints.
Correspondence and requests for materials should be addressed to C.B.
Publisher's note: Springer Nature remains neutral with regard to jurisdictional claims in published maps and institutional affiliations.